New Spectral History and Rod History Correction Method using Indicator Isotopes

Sung Hyun Cho [1], Woo Jin Lee [1], Jooil Yoon [2*], Ser Gi Hong [1*]
[1]*Department of Nuclear Engineering, Hanyang University, 222 Wangsimni-ro, Seongdong-gu, Seoul 04763, Korea*
[2]*KEPCO International Nuclear Graduate School, 658-91 Haemaji-ro, Seosaeng-myeon, Ulju-gun, Ulsan 45014, Korea*
**Corresponding author: [1*]hongsergi@hanyang.ac.kr, [2*]jiyoon@kings.ac.kr*

**Keywords: spectral history, homogenized cross section, cross-section functionalization, control rod depletion, i-SMR*

1. Introduction

In the conventional two-step procedure, a lattice transport code produces a few-group homogenized cross section library for each type of fuel assemblies, and a nodal diffusion code reconstructs the cross sections in the whole-core calculation. In general, the library is generated from a single nominal depletion calculation at the reference condition (i.e., core-averaged operating conditions), with branch calculations to consider the variation from the nominal conditions.

In a whole-core depletion problem, however, the depletion conditions of each fuel assembly vary in space and time. Fuels depleted under a different spectrum can reach the same burnup with a different nuclide inventory, and thus with different homogenized cross sections. The nominal depletion and branch calculations alone cannot represent this spectral history effect, even when the major isotopes are explicitly tracked by micro-depletion. Thus, the error grows as the off-nominal depletion continues and persists even after the conditions return to nominal.

Several correction methods have been proposed to address this problem. Bilodid and Mittag [1] used the local ^{239}Pu concentration as a spectral history indicator. Because the actinide isotope density deviations from the nominal depletion are strongly correlated with one another, a single nuclide can represent the whole inventory, and a simple correction based on the relative ^{239}Pu concentration recovers most of the history effect. Szames and Tomatis [2] observed, however, that the surveyed methods all rely on a single history parameter and that none reproduces the assembly reactivity after control rod withdrawal. This limitation is critical for the innovative SMR (i-SMR), which adopts soluble boron free operation and load-following capability as design objectives [3, 4]. The i-SMR core operates with control rods inserted throughout normal operation, so rodded depletion is a common condition rather than an exceptional one. Park et al. [5] quantified the magnitude of this effect. At 80 MWd/kg, the reactivity of a rodded depletion deviates from unrodded depletion by 31,000 pcm, and burnout of the absorber material in control rods alters the rod worth by 3,000 pcm. Therefore, a general methodology is required that can correct the group constant changes caused by the composition change under various off-nominal conditions, including control rod insertion.

This study presents a new method called the Isotope-Indicator Spectral Correction (IISC), which corrects both the spectral and control rod history effects using the node composition. The composition history is represented by four indicator nuclides rather than one, fitted as a regularized linear relation and separated by control rod state. The composition dependence of the branch derivative is treated by a distinct correction term, and rod absorber material burnout is captured by the thermal fluence accumulated during rod insertion. The methodology was verified on a 17×17 Westinghouse type fuel assembly over nominal, off-nominal, and rod movement depletion histories.

2. Methodology

2.1 Derivation of correction terms

A homogenized cross section of a node is obtained by flux–volume weighting of the fine-group cross sections, and flux distribution depends on the fine-group microscopic cross-section and isotope density. The fine-group cross-sections depend on spatial and energy self-shielding, which is again governed by the nuclide composition and the instantaneous local conditions, such as temperature and control rod insertion.

Therefore, a homogenized cross section can be considered as a function of two sets of variables, the nuclide number densities and the instantaneous operational parameters. Denoting the former by the vector $\mathbf{n}$ and the latter by the vector $\mathbf{u}$, the homogenized cross section is written $\sigma(\mathbf{n}, \mathbf{u})$. Expanding about the nominal state $(\mathbf{n_0}, \mathbf{u_0})$ yields

$$\sigma(\mathbf{n},\mathbf{u}) = \sigma(\mathbf{n}_0,\mathbf{u}_0) + \frac{\partial\sigma}{\partial\mathbf{u}}\Delta\mathbf{u} + \frac{\partial\sigma}{\partial\mathbf{n}}\Delta\mathbf{n} + \Delta\mathbf{n}^T\frac{\partial^2\sigma}{\partial\mathbf{n}\partial\mathbf{u}}\Delta\mathbf{u} + R, \quad (1)$$

where $\Delta\mathbf{n} = \mathbf{n} - \mathbf{n}_0$ and $\Delta\mathbf{u} = \mathbf{u} - \mathbf{u}_0$. The traditional cross-section functionalization considers only the first two terms, the nominal depletion cross-section $\sigma(\mathbf{n_0}, \mathbf{u_0})$ at each burnup and the branch derivative $\partial\sigma/\partial$u. The third term representing the composition effect, and the fourth one representing the composition dependence of the branch derivatives themselves, are both discarded in the

traditional method. IISC restores them approximately. The third term is corrected by a spectral history correction (SC) and the fourth term by a branch derivative correction (BC). Depletion of the rod absorber (RD) does not appear in Eq. (1), since the absorber nuclides are not explicitly tracked in nodal diffusion code. The reconstructed cross section is then

$$\sigma_{IISC} = \sigma_{base} + \Delta\sigma_{br}(\mathbf{u}) + \Delta\sigma_{BC}(\mathbf{u},\mathbf{n}) + \Delta\sigma_{SC}(\mathbf{n}) + \Delta\sigma_{RD}. \quad (2)$$

The cross sections are tabularized along burnup B, energy group, reaction type, and nuclide. However, such indices are omitted in Eq. (2), since the procedure below is applied identically for every index.

2.2 Spectral history correction

The spectral history correction relates the change of a group constant to the deviation of the indicator isotope densities through a coefficient vector **b**, determined by minimizing

$$\|\mathbf{Nb} - \mathbf{r}\|^2, \quad (3)$$

where **N** collects the indicator isotope density deviations and **r** the corresponding cross-section residuals of the m off-nominal depletion cases.

$$\mathbf{n}_l = \begin{bmatrix} N_{Xe135} \\ N_{Sm149} \\ \ln N_{Pu239} \\ N_{U235} \end{bmatrix}, \qquad \mathbf{N} = \begin{bmatrix} (\mathbf{n}_1 - \mathbf{n}_0)^T \\ (\mathbf{n}_2 - \mathbf{n}_0)^T \\ \vdots \\ (\mathbf{n}_m - \mathbf{n}_0)^T \end{bmatrix}, \quad (4)$$

$$\mathbf{r} = \begin{bmatrix} r_1 \\ r_2 \\ \vdots \\ r_m \end{bmatrix}, \quad r_l = \tilde{\sigma}_l - \left(\sigma_l + \sum_u \frac{\partial\sigma}{\partial u}\Delta u + \Delta\sigma_{BC} + \Delta\sigma_{RD} \right). \quad (5)$$

Here $\mathbf{n}_l$ is the indicator composition of case l, n_0 is the composition of the nominal unrodded depletion at the same burnup, and r_l is the corresponding residual. $\tilde{\sigma}_l$ is the cross-section from off-nominal depletion library, and σ_l is the cross-section from the nominal depletion library.

Among indicator nuclides, the logarithm of the ^{239}Pu density is used because its concentration saturates with burnup. Additional indicators are not employed, for two reasons. First, the depletion chain couples the nuclide concentrations strongly, so additional indicators provide little independent information. Second, the number of off-nominal libraries must be at least the number of indicators, so every added indicator increases the required number of lattice calculations.

The residuals are obtained from the cross-section difference between the off-nominal depletion libraries and the nominal library. An off-nominal depletion, by definition, has different instantaneous conditions from the nominal depletion. Therefore, this cross-section difference inevitably contains the branch response and cannot capture the effect of composition change alone. Furthermore, the branch derivative themselves also vary with the composition, and rodded histories additionally include the burnout of the absorber. Removing these three contributions isolates the pure composition effect.

The first row of **N** is the nominal state with zero residual, which forces the correction to vanish at nominal composition. Each column is divided by its largest absolute deviation, since the indicator densities differ by orders of magnitude and would otherwise be weighted by their units. Additionally, the indicator concentrations are strongly coupled through the depletion chain, so the columns of **N** are nearly parallel and the least-squares problem is ill-conditioned. To mitigate this problem, Tikhonov regularization is applied.

$$\mathbf{b} = \underset{\mathbf{b}}{\operatorname{argmin}}\{\|\mathbf{Nb} - \mathbf{r}\|^2 + \lambda^2\|\mathbf{b}\|^2\}, \quad \lambda > 0. \quad (6)$$

The penalty leaves the well-determined part of the solution essentially unchanged while strongly reducing the poorly determined part. The regularized problem is solved through the singular value decomposition of **N**.

$$\mathbf{N} = \mathbf{USV}^T, \quad (7)$$

$$\mathbf{b} = \mathbf{V}(\mathbf{S}^2 + \lambda^2\mathbf{I})^{-1}\mathbf{SU}^T\mathbf{r} = \sum_{k=1}^{p} \frac{s_k}{s_k^2 + \lambda^2}(\mathbf{u}_k^T\mathbf{r})\mathbf{v}_k. \quad (8)$$

where $\mathrm{s}_1 \geq \ldots \geq \mathrm{s}_\mathrm{p}$ are the singular values. The regularization strength is set relative to the largest singular value, $\lambda = \eta \mathrm{s}_1$, so that the solution is invariant under a scaling of N. The result is not sensitive to the precise value. For η between 0.01 and 0.03 the overall error of the commercial PWR assemblies varies by less than 4 pcm, as shown in Fig. 1. A smaller value reproduces the input conditions more closely but overfits the rod-state changes, and a larger value gives the opposite behavior. In this work η is set to 0.03.

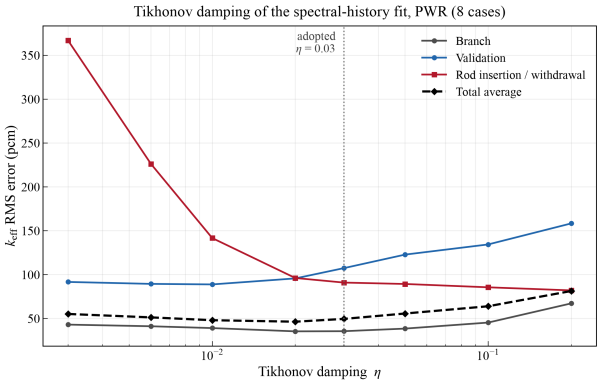


Fig. 1. RMS reactivity error as a function of the Tikhonov damping factor η

Finally, control rod insertion strongly perturbs the neutron spectrum, so the cross-section change to the same composition deviation differs with the current rod state. Therefore, cases with the rod withdrawn and

inserted are fitted separately, giving two coefficient sets $\mathbf{b}_0$ and $\mathbf{b}_1$. In the nodal calculation, spectral history correction term is reconstructed from the node composition difference, coefficient vector $\mathbf{b}$, and the rod insertion fraction f_{rod}.

$$\Delta\sigma_{SC} = [\mathbf{b}_0 + f_{rod}(\mathbf{b}_1 - \mathbf{b}_0)]^T(\mathbf{n}_{node} - \mathbf{n}_0). \quad (9)$$

2.3 Branch derivative correction

The branch derivative themselves depend on the material composition, most notably on whether the fuel was depleted with or without the control rod. Branch calculations for every off-nominal depletion would be expensive, so they are added only for the rodded depletion. The single additional library allows only one degree of freedom. Consequently, the branch coefficient correction uses a single composition coordinate, and ln N_{Pu239} is adopted since it best represents the spectral history. The sensitivity of the branch derivative to this coordinate is obtained by

$$\frac{\partial}{\partial \ln N_{Pu239}}\left(\frac{\partial\sigma}{\partial u}\right) \approx \frac{\left(\frac{\partial\sigma}{\partial u}\right)_{\text{rodded}} - \left(\frac{\partial\sigma}{\partial u}\right)_{\text{ref}}}{\ln N_{Pu239,\text{rodded}} - \ln N_{Pu239,\text{ref}}}. \quad (10)$$

The nodal calculation reconstructs the correction from the stored sensitivity, the deviation of the instantaneous parameters, and the deviation of the node ^{239}Pu density from the reference.

$$\Delta\sigma_{BC} = \Delta \ln N_{Pu239} \sum_a \frac{\partial^2\sigma}{\partial \ln N_{Pu239}\,\partial u_a}\Delta u_a. \quad (11)$$

2.4 Control rod depletion correction

When a control rod remains inserted during depletion, the absorber itself burns out. The nodal diffusion code, however, does not track the absorber nuclides, so this effect requires an additional variable. In this study, the thermal fluence is chosen, which directly measures how long the absorber has been exposed to the flux.

The effect of absorber burnout is then isolated by comparing two depletions that share the same history. Consider one depletion case in which the absorber depletes normally, and another in which rod remains fresh (F = 0). Their difference at each burnup B, evaluated at the reference fluence $F_{ref}(B)$ of the rodded nominal depletion, defines the correction as a correction curve as a function of thermal fluence.

$$\Delta\sigma_{RD}^{lib}\left(F_{ref}(B)\right) = \sigma_{rodded}(B) - \sigma_{rodded}^{fresh}(B). \quad (12)$$

The nodal calculation evaluates this curve at the node fluence and at that of the reference trajectory, and applies the difference,

$$\Delta\sigma_{RD} = \Delta\sigma_{RD}^{lib}(F_{node}) - \Delta\sigma_{RD}^{lib}\left(F_{ref}(B)\right). \quad (13)$$

3. Results

3.1 Core design

The method was applied to a Westinghouse 17×17 type fuel assembly for the i-SMR, loaded with 4.95 wt% enriched UO_2 fuel and HIGA burnable absorber rods. The control rod material is AIC. Lattice calculations were performed with DeCART2D [6] from 0 to 72 MWd/kgHM. The depletion conditions used for the library generation and for the validation are summarized in Fig. 2.

Input libraries (Total 9)		Validation libraries (Total 16)	
Nominal	T_m 580 K, T_f 900 K, Boron 10 ppm	Off-nominal	Boron 10 ppm / 1500 ppm T_f 630 K, 10% P_r T_f 825 K, 75% P_r T_m 560 K / T_m 600 K
Rodded nominal	T_m 580 K, T_f 900 K, Boron 10 ppm		
Rodded nominal	Fresh rod	Rodded Off-nominal	Boron 10 ppm / 1500 ppm T_f 630 K, 10% P_r T_f 825 K, 75% P_r T_m 560 K / T_m 600 K
Off-nominal	T_f 750 K, 25% P_r T_m 560 K / T_m 600 K		
Rodded off-nominal	T_f 750 K, 25% P_r T_m 560 K / T_m 600 K	Rod withdrawal / insertion / load-follow	

Fig. 2. Depletion conditions for the library generation and validation.

The nodal diffusion and depletion calculations were performed with RASBERY, an in-house three-dimensional core analysis code being developed at Hanyang University. RASBERY employs the semi-analytic nodal method (SANM) [7] with CMFD acceleration. The depletion is solved by the Chebyshev rational approximation method (CRAM) [8] with a constant extrapolation–linear interpolation (CELI) predictor–corrector scheme. The group constants are processed by the CHIFFON code, which reconstructs the homogenized cross sections from the DeCART2D homogenized group constant library and performs the fitting of the IISC coefficients.

3.2 Calculation results

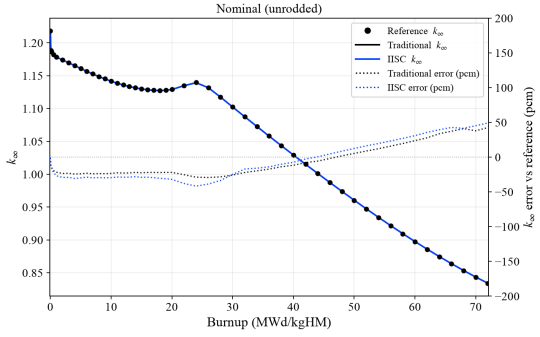


Fig. 3. Infinite multiplication factor and errors as a function of burnup for the unrodded nominal depletion case

Figs. 3 and 4 show the nominal unrodded and rodded depletions, respectively. The unrodded nominal depletion is the condition from which the traditional library is generated, and the two methods (i.e., IISC and the conventional method) give almost the same result. The RMS error of k∞ is 22 pcm for the traditional method and 28 pcm for IISC, with a maximum deviation of 54 pcm. This difference is not a history error but the difference between the DeCART2D lattice solution and the RASBERY reconstruction, and it therefore represents the baseline difference for all the other scenarios.

For the rodded nominal depletion (Fig. 4), the traditional method gives an RMS error of 340 pcm and a maximum deviation of 914 pcm, while IISC reduces them to 36 pcm and 98 pcm, respectively. The degradation is the largest at the gadolinia burnout, because the rodded spectrum delays the gadolinia burnout and shifts the reactivity peak.

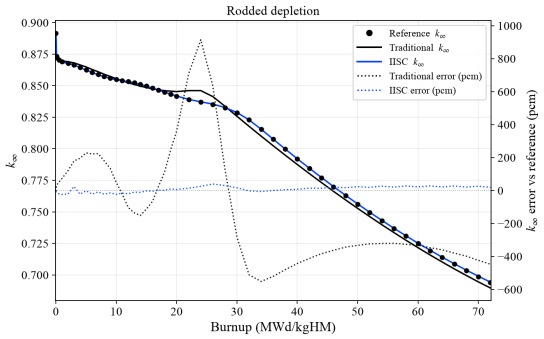


Fig. 4. Infinite multiplication factor and errors as a function of burnup for the rodded nominal depletion case.

The combined condition, in which the boron concentration is 10 ppm, T_{mod} is 540 K, and T_{fuel} is 700 K, was selected as the representative validation case. The unrodded and rodded depletions are shown in Figs. 5 and 6, respectively. For the unrodded depletion, the RMS error is reduced from 814.8 to 157.7 pcm and the maximum from 1330.7 to 353.3 pcm. For the rodded depletion, the RMS and maximum errors are reduced from 1022.0 to 81.7 pcm and from 1597.1 to 165.2 pcm, respectively.

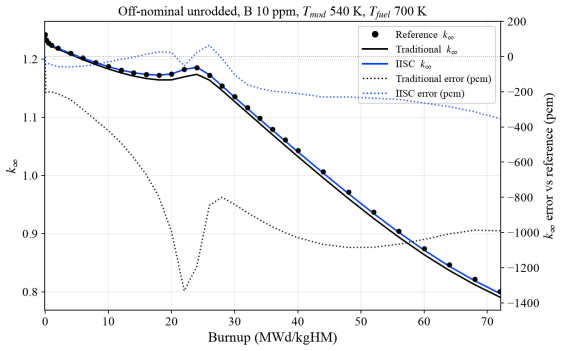


Fig. 5. Infinite multiplication factor and errors as a function of burnup for the off-nominal unrodded depletion case

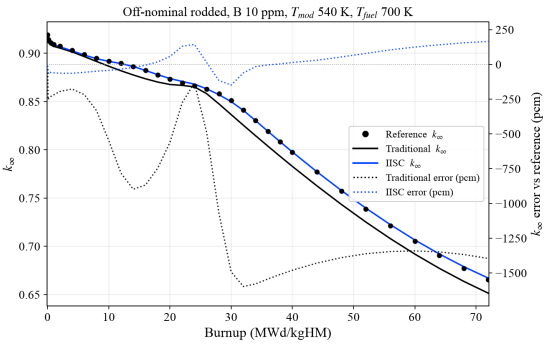


Fig. 6. Infinite multiplication factor and errors as a function of burnup for the off-nominal rodded depletion case

Finally, three rod movement histories were examined. The rod insertion, rod withdrawal, and load-follow cases are shown in Figs. 7, 8, and 9, respectively. For the rod insertion case, the RMS error is reduced from 233.1 to 64.1 pcm, and for the withdrawal case from 580.5 to 135.1 pcm. In particular, the maximum error of the rod withdrawal case decreases drastically from 1489.8 to 312.3 pcm. In the load-following operation, the control rod is inserted and withdrawn repeatedly, so every state carries a partially rodded history. The traditional method gives an RMS error of 962.1 pcm with a maximum of 2621.5 pcm, whereas IISC gives 180.1 and 815.6 pcm, respectively. The remaining error is concentrated near 28 MWd/kgHM, where the rodded spectrum delays the gadolinia burnout.

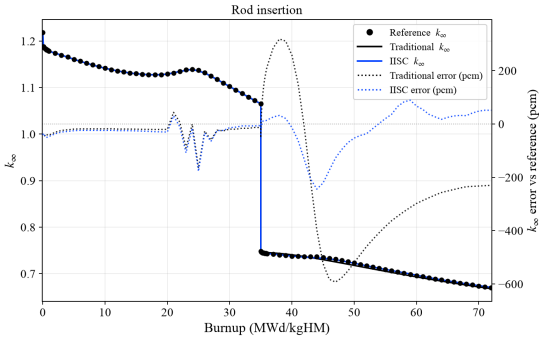


Fig. 7. Infinite multiplication factor and errors as a function of burnup for the rod insertion history case.

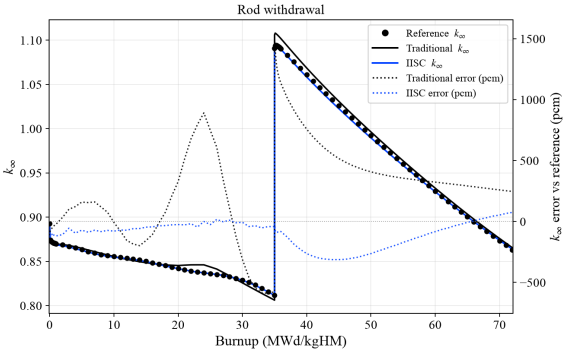


Fig. 8. Infinite multiplication factor and errors as a function of burnup for the rod withdrawal history case.

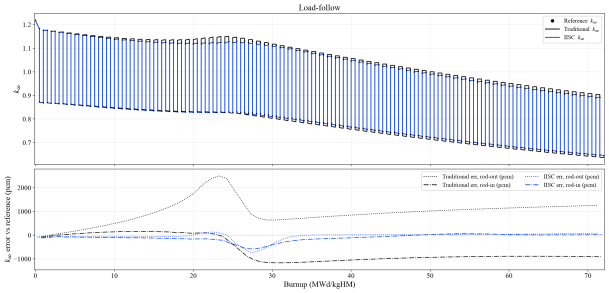


Fig. 9. Infinite multiplication factor and errors for the load-follow operation case

Fig. 10 summarizes the validation k_∞ RMS errors. IISC recovers the reference level of the reconstructed group constants for every depletion history included in the library, and keeps the RMS error within about 200 pcm for all validation cases. The remaining error is governed by the gadolinia burnout region, where the lumped Gd treatment loses information that the four indicator densities cannot recover.

4. Conclusions

In this work, the Isotope-Indicator Spectral Correction (IISC) methodology was suggested to reflect the spectral and control rod depletion histories in the reconstruction of homogenized cross sections, and it was evaluated on a 17×17 i-SMR type fuel assembly with gadolinia-bearing fuel. The composition history is carried by four indicator nuclides fitted with Tikhonov regularization and separated by control rod state, the composition dependence of the branch coefficients by a ^{239}Pu sensitivity. Rod absorber material burnout is corrected by the thermal fluence accumulated while the rod is inserted.

It was shown that IISC successfully reduced k_∞ RMS error within about 200 pcm for all the validation cases. In particular, rodded depletion and load-follow operation case exhibited drastic error reduction. The remaining error is mainly in the gadolinia burnout region, where the lumped Gd treatment cannot resolve the state of the absorber. Future work will focus on three-dimensional whole-core calculations to assess the applicability of IISC to practical i-SMR core analysis.

ACKNOWLEDGEMENT

This work was supported by the Nuclear Safety Research Program through the Regulatory Research Management Agency for SMRs (RMAS) and the Nuclear Safety and Security Commission (NSSC) of the Republic of Korea (No. RS-2024-00509678).

REFERENCES

[1] I. Bilodid and S. Mittag, “Use of the local Pu-239 concentration as an indicator of burnup spectral history in DYN3D,” Annals of Nuclear Energy, Vol. 37, No. 9, pp. 1208–1213, 2010, doi: 10.1016/j.anucene.2010.04.019.

[2] E. Szames and D. Tomatis, “A review of history parameters in PWR core analysis,” Nuclear Engineering and Design, Vol. 347, pp. 158–174, 2019, doi: 10.1016/j.nucengdes.2019.03.012.

[3] H. O. Kang, B. J. Lee, and S. G. Lim, “Light water SMR development status in Korea,” Nuclear Engineering and Design, Vol. 419, Art. no. 112966, 2024, doi: 10.1016/j.nucengdes.2024.112966.

[4] S. H. Cho, W. J. Lee, and S. G. Hong, “Neutronic design and analysis of a soluble boron-free small modular reactor core with GdN-CBA burnable absorber rods for load-following operations,” Annals of Nuclear Energy, Vol. 214, 111203, 2025, doi: 10.1016/j.anucene.2025.111203.

[5] J. Park, W. Kim, Y. Kang, and D. Lee, “Development of Control Rod Depletion Methodology for non-Boron Operation of SMR,” Transactions of the Korean Nuclear Society Spring Meeting, Jeju, Korea, May 9–10, 2024.

[6] J. Y. Cho et al., “DeCART2D v1.1 User’s Manual,” KAERI/UM-40/2016, Korea Atomic Energy Research Institute, 2016.

[7] V. G. Zimin and H. Ninokata, “Nodal neutron kinetics model based on nonlinear iteration procedure for LWR analysis,” Annals of Nuclear Energy, Vol. 25, No. 8, pp. 507–528, 1998, doi: 10.1016/S0306-4549(97)00078-9.

[8] M. Pusa, “Rational Approximations to the Matrix Exponential in Burnup Calculations,” Nuclear Science and Engineering, Vol. 169, No. 2, pp. 155–167, 2011, doi: 10.13182/NSE10-81.